HHS Public Access

Author manuscript

Retina. Author manuscript; available in PMC 2019 November 01.

Published in final edited form as:

Retina. 2018 November ; 38(11): 2214–2219. doi:10.1097/IAE.0000000000001841.

Hyper-Reflective Deposition in the Background of Advanced Stargardt Disease

Lyam Ciccone[1], **Winston Lee**[1], **Jana Zernant**[1], **Koji Tanaka**[1], **Kaspar Schuerch**[1], **Stephen H. Tsang**[1,2], and **Rando Allikmets**[1,2,*]

[1]Department of Ophthalmology, Columbia University, New York, NY

[2]Department of Pathology & Cell Biology, Columbia University, New York, NY

Abstract

Purpose—To describe an unusual manifestation of hyper-reflective deposits in the subretinal space in a group of clinically and genetically confirmed Stargardt disease patients.

Methods—Retrospective review of color fundus, autofluorescence (AF), infrared reflectance (IR), red-free (RF) images and spectral domain-optical coherence tomography (SD-OCT) in 296 clinically diagnosed and genetically confirmed (2 expected disease-causing mutations in *ABCA4*) patients with Stargardt disease. Full-field electroretinogram (ffERG), medical history and genotype data (*in silico* predictions) were further analyzed from the selected cohort.

Results—Eight out of 296 patients (2.7%) were found to exhibit small crystalline deposits which were detectable on certain imaging modalities such as color, IR and RF images, but not AF. The deposits were most prevalent in the superior region of the macula and SD-OCT revealed their presence in the subretinal space. All patients presented with these findings at a notably advanced disease stage with abnormal ffERG and a high proportion of highly deleterious *ABCA4* alleles.

Conclusion—Hyper-reflective subretinal deposits may be a manifestation of advanced ABCA4 disease, particularly in regions susceptible to disease-related changes such as lipofuscin accumulation.

Keywords

ABCA4; Hyper-reflective deposits; Stargardt; Subretinal; Superotemporal

Introduction

Recessive Stargardt disease (STGD1) is the most common form of inherited, juvenile-onset retinal dystrophy affecting approximately 1 in 10,000 people worldwide.[1] Since its discovery as the causative gene for STGD1, over 1,000 mutations have been reported in the ATP Binding Cassette Subfamily A Member 4 (*ABCA4*) gene[2] which produce a large spectrum of phenotypes ranging from bull's eye-maculopathy[3, 4] to retina-wide

*Corresponding Author: Rando Allikmets, Ph.D., Department of Ophthalmology, Eye Research Annex Rm 202, 160 Ft Washington Ave, New York, NY 10032, rla22@cumc.columbia.edu.

Competing Interests: None declared

degeneration.[5, 6] Despite such extensive clinical heterogeneity, ABCA4-associated diseases exhibit a well-defined profile of pathognomonic features which include the development and accumulation of yellow, pisciform-shaped foci (flecks)[7, 8] and sparing of the peripapillary region,[9] among others.

A more expanded profile includes characteristics associated with specific sub-groups or progressive stages within the disease. For instance, RPE pigment migration[10] and choroidal sclerosis[11] are features associated with advanced disease stages while external limiting membrane thickening[12] and fine, reflective dots in the central macula[13] have been described in younger patients. Documenting phenotypic spectrum of a disease increases diagnostic accuracy and provides insight into disease etiology.

Here we describe an infrequent but discernable clinical manifestation of hyper-reflective depositions in the macula and midperipheral retina in a group of patients diagnosed with advanced, genetically confirmed Stargardt disease.

Methods

All patients were enrolled under the protocol #AAAI9906 approved by the Columbia University Medical Center Institutional Review Board. All procedures adhered to tenets set out in the Declaration of Helsinki. A retrospective review of clinical data from 296 genetically confirmed patients with Stargardt disease was performed. Patients included in the initial cohort underwent a complete ophthalmic examination by a retinal specialist (S.H.T) including slit-lamp examination, dilated fundus examination and measurement of best-corrected visual acuity (BCVA). All patients were diagnosed with Stargardt disease and harbored at least two (as expected for a recessive disease) *ABCA4* mutations detected by direct sequencing of all 50 exons and flanking intronic regions in the *ABCA4* gene as previously described.[14, 15]

Clinical data for all patients included color and red-free fundus photos acquired by a FF 450plus Fundus Camera (Carl Zeiss Meditec AG, Jena, Germany), autofluorescence (488-nm excitation) images and spectral domain-optical coherence tomography (SD-OCT) acquired with a Spectralis HRA+OCT module (Heidelberg Engineering, Heidelberg, Germany). In most, but not all patients, full-field electroretinogram (ffERG) results were available and included. Ganzfeld full-field electroretinograms (ERGs) for each patient were recorded using the Diagnosys Espion Electrophysiology System (Diagnosys LLC, Littleton, MA, USA). Recordings were performed according to International Society for Clinical Electrophysiology of Vision (ISCEV) standards and guidelines.[16]

Results

A review of 296 clinically-diagnosed and genetically confirmed patients with Stargardt disease revealed a small fraction of cases (n=8, 2.7%) who presented with an unusual distribution of reflective yellow spots on fundoscopy and color fundus photos (Figure 1A). The deposits were distributed in a nonspecific pattern across the macula and midperiphery but were discernably more prevalent in the supero-temporal region. The spots appeared to be largely round in shape but varied in size from 50–70 μm. Distinct from yellow, pisciform

flecks which represent lipofuscin accumulation and, therefore, produce an autofluorescence signal, these spots were only visible on reflective imaging modalities (color and red-free fundus photographs, near-infrared reflectance and optical coherent tomography scans) and did not yield a detectable autofluorescence signal in the 488-nm range (SW-AF) (Figure 1B). Furthermore, these deposits exhibit a hard, concrete appearance, which is different from the faint hue of the lipofuscin-derived flecks in the RPE. Correlations to these deposits in fundus images were found on SD-OCT sections which revealed discrete, reflective granules of varying sizes in the subretinal space, specifically at the anterior side of the RPE layer (Figure 2). The granules were not visible in any other retinal layers.

Demographic, clinical and genetic characteristics of the cohort are summarized in Table 1. Mean age of the cohort is 38.7 years, ranging between 26–57 years. No significant systemic history was noted with the exception of P3 who reported a history of hypertension. All except two patients reported visual symptoms within the first decade of life. Best-corrected visual acuity (BCVA) were predominantly poor, from 20/300 to counting fingers (CF) except P8 who was measured to be 20/100 and 20/30, OD and OS, respectively. Interestingly, all patients presented at relatively advanced stages of Stargardt disease. Features associated with ‘classical’ Stargardt disease were observed in autofluorescence imaging, (Figure 1B) including peripapillary sparing and heterogeneous patterns of flecks across the posterior pole. Full-field electroretinography (ffERG) were analyzed in all patients except for P3 for whom data were not available. All cases exhibited generalized cone dysfunction while P1, P3, P4 and P8 had also marginal to severe decreases in rod function.

In accordance with the advanced phenotypes, the *ABCA4* genetic profile of the cohort consisted of deleterious variants across different classes of mutations including a small deletion/frame-shift variant, p.T1346Gfs*75, in P2 and several strong deleterious missense variants, p.P1380L and p.T1526M. As well as others including p.R2107H which is associated with African-American patients.[17] Two variants in canonical splice sites, c.6386+2C>G and c.4540-2A>G, were predicted to abolish splicing. The c.5461-10T>C variant found in P5 has been shown to cause exon skipping.[18]

Discussion

The progressive accumulation of numerous yellow flecks across the retina is a characteristic feature of Stargardt disease. The autofluorescence signal and subretinal localization of these flecks denotes a connection to lipofuscin and in fact, it has been suggested that they represent lipofuscin-engorged RPE cells, displaced and stacked RPE, remnants of RPE cell lysis or a byproduct of ongoing photoreceptor degeneration in the subretinal space.[7, 19, 20] The reflective deposits described in this cohort were similarly found in the subretinal space and yellow on fundoscopy and color fundus photos, but differed in appearance and did not exhibit an autofluorescence signal. The deposits exhibit a round conformation and a rather solid appearance compared to the fluid and pyramidal-like appearance of flecks. Other forms of deposition in the macula of Stargardt disease patients have been described. Fujinami et al. reported the observation of fine macula dots in a subset childhood onset cases; however

these dots are recognizably distinct from the deposition described in this study in that they are visible on AF and exhibit a different manifestation on OCT.[13]

The actual composition of the reflective deposits is not known; however, because of its presence in Stargardt disease patients, a connection to lipofuscin accumulation and ABCA4 pathology may exist. Furthermore, previous studies utilizing quantitative autofluorescence have identified an increased presence of lipofuscin in the superotemporal region.[21] This is especially interesting given the observation that the reflective deposits have a spatial preference for the superotemporal region as well. Deposition in this region may be a visual manifestation related to RPE damage based on previous observations that suggest a susceptibility of these cells in the superotemporal region. A vascular connection to the origin of these deposits may also be plausible as they bear an apparent resemblance to hard exudates found in vascular diseases. Histological analyses have characterized the composition of these hard exudates as containing lipid-laden macrophages and other proteinaceous substances which may be attributable to the etiology of lipofuscin in ABCA4 disease.[22–24] Contributions from underlying vessels may also be possible as choroidal alterations have been reported in the course ABCA4 disease.[11, 25–27] Precise spatial correlations in the retina between the regions of deposition and choroidal thinning cannot be made, however; both were found to be evident features in the advanced stages of disease.

Several diseases have been associated with the retinal manifestation of crystalline deposition, ranging from genetic diseases related to enzyme deficiencies including primary hyperoxalosis,[28] cystinosis,[29] hyperornithinemia,[30] Sjögren-Larsson syndrome,[31, 32] drug induced retinopathies (Tamoxifen,[33, 34] Nitrofurantoin,[35] Talc[36, 37]), primary ocular pathologies like Bietti's Crystalline Retinopathy[38–40] or long standing retinal detachments.[41] It is unlikely that the deposits are associated with a co-existing condition (including those listed above) in this cohort given the negative medical history. They may rather represent an incidental complication associated with advanced disease stage.[42]

This report expands the clinical spectrum of the ABCA4 disease, presenting an infrequent but notable prevalence of hyper-reflective deposition in the subretinal space. The deposits are apparent in 2–3% of cases, localize at the superior region of the macula and are found at an advanced disease stage. It is unclear whether these deposits are directly associated with the pathogenesis of ABCA4 dysfunction or are analogous to similar manifestations in other diseases which affect the underlying choroidal or retinal vasculature.

Acknowledgments

Financial Support: This work was supported, in part, by grants from the National Eye Institute/NIH EY021163, EY019861 and EY019007 (Core Support for Vision Research), and unrestricted funds from Research to Prevent Blindness (New York, NY) to the Department of Ophthalmology, Columbia University.

References

1. Blacharski PA. Fundus flavimaculatus. In: Newsome DA, editorRetinal Dystrophies and Degenerations. New York: Raven Press; 1988. 135–159.
2. Allikmets R, et al. A photoreceptor cell-specific ATP-binding transporter gene (ABCR) is mutated in recessive Stargardt macular dystrophy. Nat Genet. 1997; 15:236–246. [PubMed: 9054934]

3. Duncker T, et al. Quantitative fundus autofluorescence distinguishes ABCA4-associated and non-ABCA4-associated bull's-eye maculopathy. Ophthalmology. 2015; 122:345–355. [PubMed: 25283059]
4. Cella W, et al. G1961E mutant allele in the Stargardt disease gene ABCA4 causes bull's eye maculopathy. Exp Eye Res. 2009; 89:16–24. [PubMed: 19217903]
5. Klevering BJ, et al. Phenotypic spectrum of autosomal recessive cone-rod dystrophies caused by mutations in the ABCA4 (ABCR) gene. Invest Ophthalmol Vis Sci. 2002; 43:1980–1985. [PubMed: 12037008]
6. Maugeri A, et al. Mutations in the ABCA4 (ABCR) gene are the major cause of autosomal recessive cone-rod dystrophy. Am J Hum Genet. 2000; 67:960–966. [PubMed: 10958761]
7. Sparrow JR, et al. Flecks in Recessive Stargardt Disease: Short-Wavelength Autofluorescence, Near-Infrared Autofluorescence, and Optical Coherence Tomography. Invest Ophthalmol Vis Sci. 2015; 56:5029–5039. [PubMed: 26230768]
8. Cukras CA, et al. Centrifugal expansion of fundus autofluorescence patterns in Stargardt disease over time. Arch Ophthalmol. 2012; 130:171–179. [PubMed: 21987580]
9. Cideciyan AV, et al. ABCA4-associated retinal degenerations spare structure and function of the human parapapillary retina. Invest Ophthalmol Vis Sci. 2005; 46:4739–4746. [PubMed: 16303974]
10. Mullins RF, et al. Autosomal recessive retinitis pigmentosa due to ABCA4 mutations: clinical, pathologic, and molecular characterization. Invest Ophthalmol Vis Sci. 2012; 53:1883–1894. [PubMed: 22395892]
11. Bertelsen M, et al. Generalized choriocapillaris dystrophy, a distinct phenotype in the spectrum of ABCA4-associated retinopathies. Invest Ophthalmol Vis Sci. 2014; 55:2766–2776. [PubMed: 24713488]
12. Lee W, et al. The external limiting membrane in early-onset Stargardt disease. Invest Ophthalmol Vis Sci. 2014; 55:6139–6149. [PubMed: 25139735]
13. Fujinami K, et al. Fine central macular dots associated with childhood-onset Stargardt Disease. Acta Ophthalmol. 2014; 92:e157–159.
14. Zernant J, et al. Analysis of the ABCA4 genomic locus in Stargardt disease. Hum Mol Genet. 2014; 23:6797–6806. [PubMed: 25082829]
15. Zernant J, et al. Analysis of the ABCA4 gene by next-generation sequencing. Invest Ophthalmol Vis Sci. 2011; 52:8479–8487. [PubMed: 21911583]
16. McCulloch DL, et al. ISCEV Standard for full-field clinical electroretinography (2015 update). Doc Ophthalmol. 2015; 130:1–12.
17. Zernant J, et al. Genetic and clinical analysis of ABCA4-associated disease in African American patients. Hum Mutat. 2014; 35:1187–1194. [PubMed: 25066811]
18. Sangermano R, et al. Photoreceptor Progenitor mRNA Analysis Reveals Exon Skipping Resulting from the ABCA4 c. 5461-10T-->C Mutation in Stargardt Disease. Ophthalmology. 2016; 123:1375–1385. [PubMed: 26976702]
19. Eagle RC Jr, et al. Retinal pigment epithelial abnormalities in fundus flavimaculatus: a light and electron microscopic study. Ophthalmology. 1980; 87:1189–1200. [PubMed: 6165950]
20. Lopez PF, et al. Autosomal-dominant fundus flavimaculatus. Clinicopathologic correlation. Ophthalmology. 1990; 97:798–809. [PubMed: 2374685]
21. Greenberg JP, et al. Quantitative fundus autofluorescence in healthy eyes. Invest Ophthalmol Vis Sci. 2013; 54:5684–5693. [PubMed: 23860757]
22. Toussaint D, Cogan DG, Kuwabara T. Extravascular lesions of diabetic retinopathy. Arch Ophthalmol. 1962; 67:42–47. [PubMed: 14039779]
23. Flynn E, et al. Fundus autofluorescence and photoreceptor cell rosettes in mouse models. Invest Ophthalmol Vis Sci. 2014; 55:5643–5652. [PubMed: 25015357]
24. Cusick M, et al. Histopathology and regression of retinal hard exudates in diabetic retinopathy after reduction of elevated serum lipid levels. Ophthalmology. 2003; 110:2126–2133. [PubMed: 14597519]
25. Muller PL, et al. Choroidal Alterations in Abca4-Related Retinopathy. Retina. 2017; 37:359–367. [PubMed: 27414126]

26. Yeoh J, et al. Choroidal imaging in inherited retinal disease using the technique of enhanced depth imaging optical coherence tomography. Graefes Arch Clin Exp Ophthalmol. 2010; 248:1719–1728. [PubMed: 20640437]
27. Adhi M, et al. Morphology and Vascular Layers of the Choroid in Stargardt Disease Analyzed Using Spectral-Domain Optical Coherence Tomography. Am J Ophthalmol. 2015; 160:1276–1284. e1271. [PubMed: 26314663]
28. Bullock JD, Albert DM. Flecked retina. Appearance secondary to oxalate crystals from methoxyflurane anesthesia. Arch Ophthalmol. 1975; 93:26–31. [PubMed: 1111483]
29. Read J, et al. Nephropathic cystinosis. Am J Ophthalmol. 1973; 76:791–796. [PubMed: 4748200]
30. Takki K. Gyrate atrophy of the choroid and retina associated with hyperornithinaemia. Br J Ophthalmol. 1974; 58:3–23. [PubMed: 4841281]
31. McKusick VA. A Catalog of Human Genes and Genetic Disorders. Baltimore: Johns Hopkins University Press; 1998.
32. Willemsen MA, et al. Juvenile macular dystrophy associated with deficient activity of fatty aldehyde dehydrogenase in Sjogren-Larsson syndrome. Am J Ophthalmol. 2000; 130:782–789. [PubMed: 11124298]
33. Kaiser-Kupfer MI, Lippman ME. Tamoxifen retinopathy. Cancer Treat Rep. 1978; 62:315–320. [PubMed: 647693]
34. Kaiser-Kupfer MI, Kupfer C, Rodrigues MM. Tamoxifen retinopathy. A clinicopathologic report. Ophthalmology. 1981; 88:89–93. [PubMed: 7243233]
35. Ibanez HE, Williams DF, Boniuk I. Crystalline retinopathy associated with long-term nitrofurantoin therapy. Arch Ophthalmol. 1994; 112:304–305. [PubMed: 8129651]
36. Friberg TR, Gragoudas ES, Regan CD. Talc emboli and macular ischemia in intravenous drug abuse. Arch Ophthalmol. 1979; 97:1089–1091. [PubMed: 444139]
37. AtLee WE Jr. Talc and cornstarch emboli in eyes of drug abusers. JAMA. 1972; 219:49–51. [PubMed: 5066587]
38. Francois J, De Laey JJ. Bietti's crystalline fundus dystrophy. Ann Ophthalmol. 1978; 10:709–716. [PubMed: 677651]
39. Grizzard WS, et al. Crystalline retinopathy. Am J Ophthalmol. 1978; 86:81–88. [PubMed: 677237]
40. Wilson DJ, et al. Bietti's crystalline dystrophy. A clinicopathologic correlative study. Arch Ophthalmol. 1989; 107:213–221. [PubMed: 2783846]
41. Cogan DG, et al. Calcium oxalate and calcium phosphate crystals in detached retinas. AMA Arch Ophthalmol. 1958; 60:366–371. [PubMed: 13570759]
42. Moisseiev J, et al. Superficial retinal refractile deposits in juxtafoveal telangiectasis. Am J Ophthalmol. 1990; 109:604–605. [PubMed: 2333929]

Summary statement

An unusual accumulation of hyper-reflective deposits is observed in a small fraction of patients with advanced Stargardt disease. Although the precise composition of the deposits is unknown, they were found to cluster predominantly in the superotemporal region of the macula in the subretinal space and are associated with mostly deleterious mutations in the *ABCA4* gene.

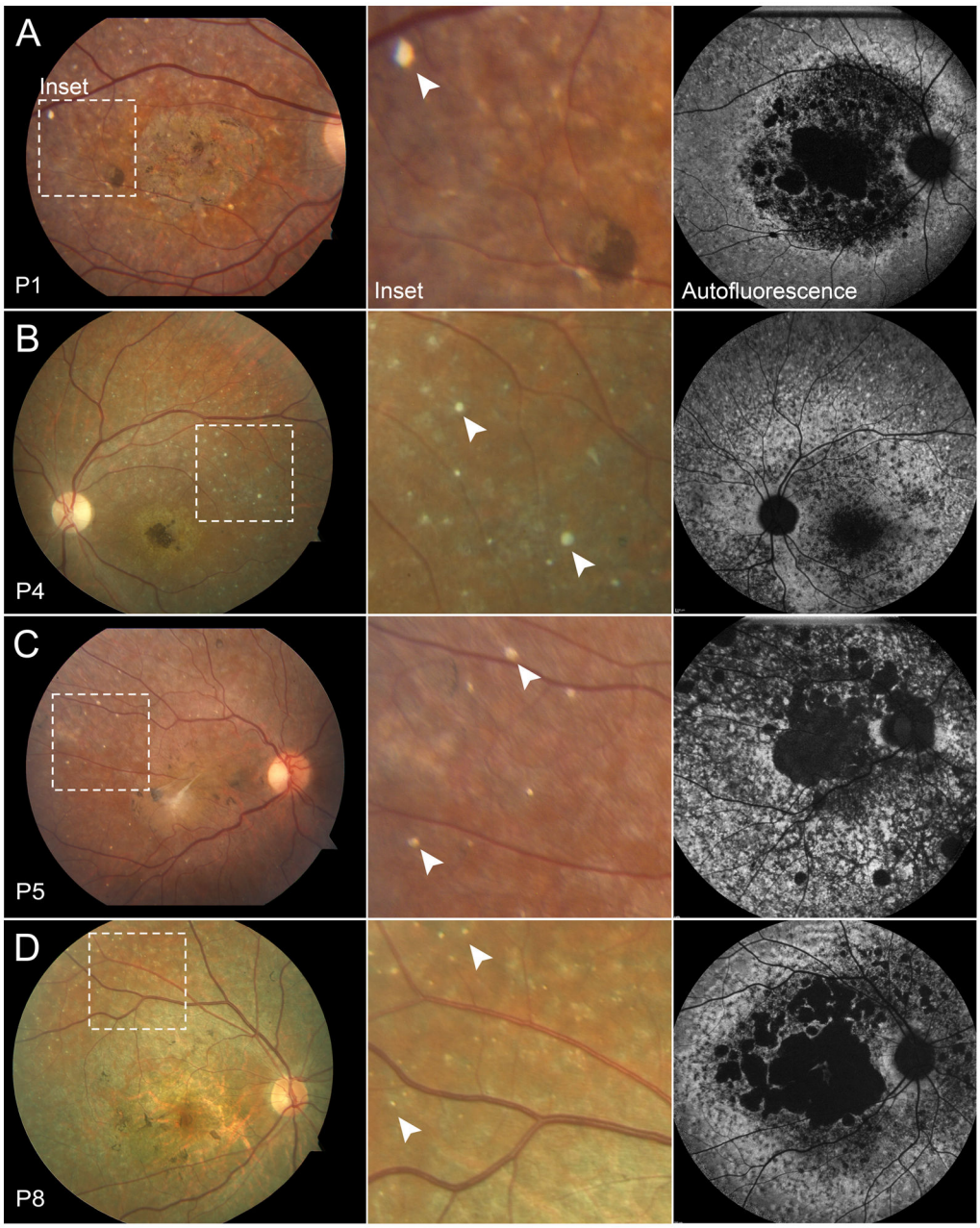

Figure 1.

Hyper-reflective deposits in color and autofluorescence in patients with Stargardt disease. Fifty-five degree color fundus photo of P1 (A), P4 (B), P5 (C) and P8 (D) with dotted insets illustrating hyper-reflective deposits (arrowheads) in the superior-temporal region of the macula. Deposits are not visible in corresponding regions on AF imaging.

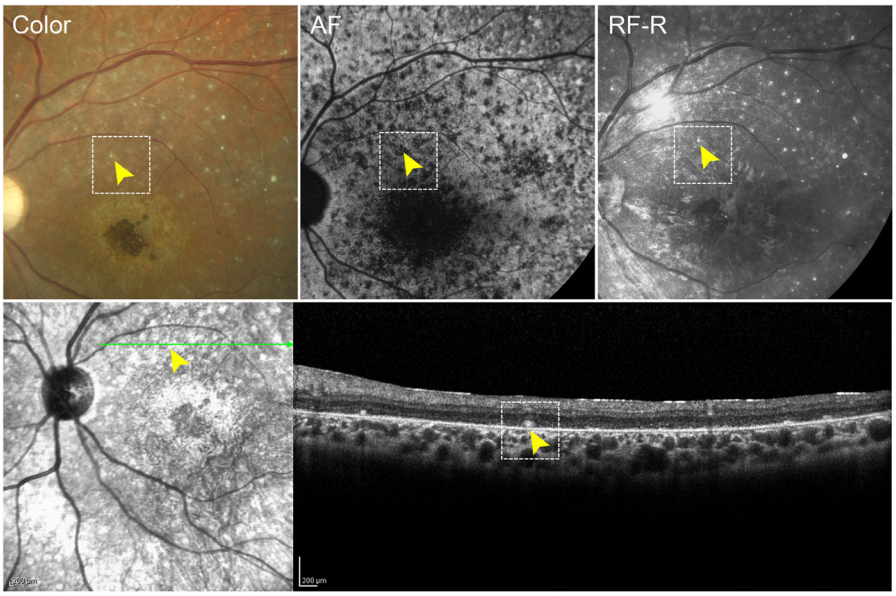

Figure 2.

Multi-modal imaging of a hyper-reflective deposit in a patient with Stargardt disease. Color, autofluorescence (AF), red-free-reflectance (RF-R) and infrared imaging of a hyper-reflective deposit (yellow arrowhead, dotted box) with corresponding spectral domain-optical coherence tomography showing localization in the subretinal space.

Table 1

Clinical, Genetic and Demographic Characteristics of Patients with Stargardt Disease and Hyper-Reflective Subretinal Deposition

Patient	Gender	Age	Age of Onset	Race/Ethnicity	BCVA		*ABCA4* Mutation 1	*ABCA4* Mutation 2	ffERG			
					OD	OS			Scotopic	Maximal	30 Hz. Flicker	Photopic
1	M	34	10	White	20/300	20/400	p.P1380L	p.P1380L	↓	↓	ND	ND
2	F	30	7	White	CF	20/400	c.4036_4037delAC	c.4036_4037delAC				
3	M	33	7	Indian	CF	20/300	IVS7:c.859-9T>C	p.Q2220*	↓↓	↓↓	ND	ND
4	F	26	10	White	CF	CF	p.T1526M	IVS46:c.6386+2C>G	↓	↓	↓↓	↓↓
5	F	38	10	White	20/400	20/400	p.P1380L	IVS38:c.5461-10T>C			↓↓	↓↓
6	F	40	19	White	20/400	20/400	p.T1526M	p.L2027F	WNL	WNL	↓↓	↓
7	M	57	10	Black	CF	CF	IVS30:c.4540-2A>G	p.R2107H			ND	ND
8	M	52	51	Asian	20/100	20/30+2	p.R24H	c.1561delG	↓	WNL	↓↓	↓

Abbreviations: M, male; F, female; BCVA, best-corrected visual acuity; OD, right eye; OS, left eye; CF, counting fingers; ffERG, full-field electroretinogram; ND, non-detectable; WNL, within normal limits (age-matched) ↓, Diminished signal; ↓↓, Very diminished signal.